Bioorganic & Medicinal Chemistry 28 (2020) 115727

Contents lists available at ScienceDirect

Bioorganic & Medicinal Chemistry

journal homepage: www.elsevier.com/locate/bmc

Focused structure-activity relationship profiling around the 2-phenylindole scaffold of a cannabinoid type-1 receptor agonist-positive allosteric modulator: site-III aromatic-ring congeners with enhanced activity and solubility

Peter C. Schaffer[a], Pushkar M. Kulkarni[a], David R. Janero[a,b], Ganesh A. Thakur[a,*]

[a] Department of Pharmaceutical Sciences, Bouvé College of Health Sciences, Northeastern University, Boston, MA 02115, United States
[b] Health Sciences Entrepreneurs, Northeastern University, Boston, MA 02115, United States

ARTICLE INFO

Keywords:
Cannabinoid type-1 receptor
Positive allosteric modulator
Physiochemical properties
Functional selectivity
2-Phenylindole

ABSTRACT

Specific tuning of cannabinoid 1 receptor (CB1R) activity by small-molecule allosteric modulators is a therapeutic modality with multiple properties inherently advantageous to therapeutic applications. We previously generated a library of unique CB1R positive allosteric modulators (PAMs) derived from GAT211, which has three pharmacophoric sites critical to its ago-PAM activity. To elaborate our CB1R PAM library, we report the rational design and molecular-pharmacology profiling of several 2-phenylindole analogs modified at the "site-III" aromatic ring. The comprehensive structure–activity relationship (SAR) investigation demonstrates that attaching small lipophilic functional groups on the *ortho*-position of the GAT211 site-III phenyl ring could markedly enhance CB1R ago-PAM activity. Select site-III modifications also improved GAT211's water solubility. The SAR reported both extends the structural diversity of this compound class and demonstrates the utility of GAT211's site-III for improving the parent compound's drug-like properties of potency and/or aqueous solubility.

1. Introduction

The mammalian endocannabinoid system (ECS) is a ubiquitous information-transducing network in which endogenous lipids (endocannabinoids) act as signaling molecules primarily by engaging the orthosteric sites of the cannabinoid type-1 (CB1R) and type-2 (CB2R) G-protein coupled receptors (GPCRs).[1–6] As the most abundant GPCR in the CNS and by virtue of its diverse functions in the periphery, CB1R helps regulate a wide range of physiological processes, from neurotransmission to energy metabolism.[4,7,8] Abnormal CB1R-dependent ECS activity is recognized as a pathogenic component of several neurological, psychiatric, cardiometabolic, and other disease states representing unsolved medical problems, making CB1R a prime therapeutic target.[9–11] Over the last several decades, extensive discovery campaigns have yielded a plethora of structurally diverse designer CB1R orthosteric ligands with biological activity. However, adverse events such as psychobehavioral problems and addiction associated with typical CB1R orthosteric (ant)agonists/inverse agonists have plagued their translation into the clinic.[2,12–14]

As an alternative to CB1R orthosteric agents, allosteric ligands are garnering interest for actualizing the pharmacotherapeutic impact of CB1R modulation.[15] The potential for allosteric modulation to circumvent the liabilities associated with typical orthosteric CB1R ligands by offering comparatively greater selectivity, tissue specificity, and safety, as well as less potential for receptor desensitization, has prompted medicinal chemistry efforts to design and profile novel CB1R allosteric effectors as candidate therapeutics.[16–18]

The 2-phenylindoles GAT211 (**33**) from this laboratory,[19] ZCZ011,[20] and its non-nitro derivative ABD1236,[21] have emerged as prototypic CB1R agonist-positive allosteric modulators ("ago-PAMs") (Figure 1). These CB1R ligands act as both a PAM and an agonist at this GPCR's allosteric site, i.e., they increase the binding and function of orthosteric agonists at CB1R while stimulating the receptor on their own.[22,23] We previously demonstrated that GAT211's ago-PAM activity reflects its enantiomers: the (*R*)-(+)- enantiomer (GAT228) is a CB1R allosteric agonist, while the (*S*)-(-)-enantiomer (GAT229) is a

Abbreviations: ago-PAM, agonist-positive allosteric modulator; CNS, central nervous system; BB, building block; ECS, endocannabinoid system; GPCR, G-protein coupled-receptor; (h)CB1R, (human) cannabinoid type-1 receptor; NAM, negative allosteric modulator; PAM, positive allosteric modulator; SAR, structure-activity relationship

* Corresponding author.
E-mail address: g.thakur@northeastern.edu (G.A. Thakur).

https://doi.org/10.1016/j.bmc.2020.115727
Received 22 May 2020; Received in revised form 6 August 2020; Accepted 19 August 2020
Available online 29 August 2020
0968-0896/

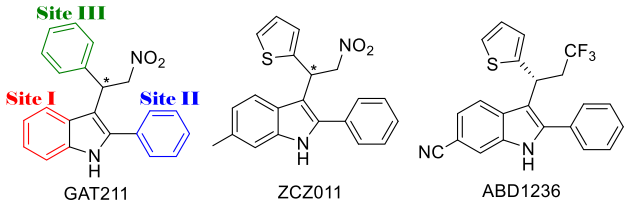

Fig. 1. 2-Pheylindole type CBIR ago-PAMs ZCZ011, ABD1236, and GAT11(with three defined sites color coded).

CB1R PAM (Figure 1).[23]

Structurally, these ago-PAMs share three principal regions potentially amenable to modification/elaboration, as designated in Figure 1 for GAT211. ZCZ011 differs from GAT211 by its 6-methyl group at site I, and our recent structure–activity relationship (SAR) study with the GAT211 scaffold identified positions 6- and 7- at site I as amenable to lipophilic-group substitution for greatly enhancing CB1R ago-PAM activity and the *ortho*-position at site III for potentially incorporating either lipophilic or hydrophilic groups.[24]

The effects of site-III substitutions on drug-like potency and physicochemical properties of 2-phenylindole CB1R ago-PAMS have not been explored in systematic detail. Both ZCZ011 and ABD1236 feature a site-III 2-thienyl ring which enhanced CB1R ago-PAM activity. However, the 2-thienyl substituent invites formation of nephrotoxic and hepatotoxic products from thiophene metabolism, the cause of market withdrawal for several drugs.[25,26] Furthermore, replacement of benzene with thiophene typically results in a slight increase in lipophilicity,[27] which exacerbates the major drawback of the 2-phenylindole class of CB1R ago-PAMs, limited aqueous solubility. This limitation, and the unfavorable physiochemical and metabolic properties associated with thiophene, justify exploring alternative site-III substituents to elaborate the GAT211-derived CB1R ago-PAM library and, more globally, define the role of site-III as determinant of the pharmacological and physicochemical properties of 2-phenylindole CB1R ago-PAMs.

We recently demonstrated the requirement of a site-III ring substituent for CB1R PAM activity of GAT211.[28] Additionally, synthesis and profiling of 2-phenylindole analogs with site-III pyridyl and monosubstituted fluorophenyl rings suggested that *ortho* substitutions in the site-III phenyl ring are favorable for activity.[24] Aside from site-III phenyl derivatives reported by our group,[19] the only other site-III ring variations published are 2-thienyl, 2-furyl, and cyclopropyl-methyl.[21] Detailed correlations between the site-III ring functionality and pharmacological activity are lacking, especially for site III five-membered heteroaromatic rings.

To address this knowledge gap, we report a comprehensive SAR study on the site-III ring within the 2-phenylindole scaffold. This study constitutes an in-depth analysis of group-size and positional-preference effects of ring substituents at site III on CB1R ago-PAM activity.

2. Results and discussion

2.1. Chemistry

All nitrovinyl building blocks (BBs) were prepared from their corresponding, commercially available aromatic aldehydes. The last step for the synthesis of all site-III analogs (**33–70**), depicted in Scheme 1, involves ammonium trifluoroacetate catalyzed C3 alkylation of 2-phenylindoles with various nitrovinyl BBs (step d). 1-pyrrolidyl substituted phenylnitrovinyl BBs, **16a-c**, were directly prepared from their corresponding aldehydes in one step under reflux conditions (step a, Scheme 1). Thiazole, oxazole, and 1-methylimidazole nitrovinyl BBs, **31a-e**, were prepared by a two-step process starting with a Henry reaction (step b) to form the nitroalcohol intermediate which subsequently underwent dehydration (step c) to yield the desired nitrovinyl BB.[29] In limited instances, 6-methyl-2-phenylindole (**32**), prepared directly from

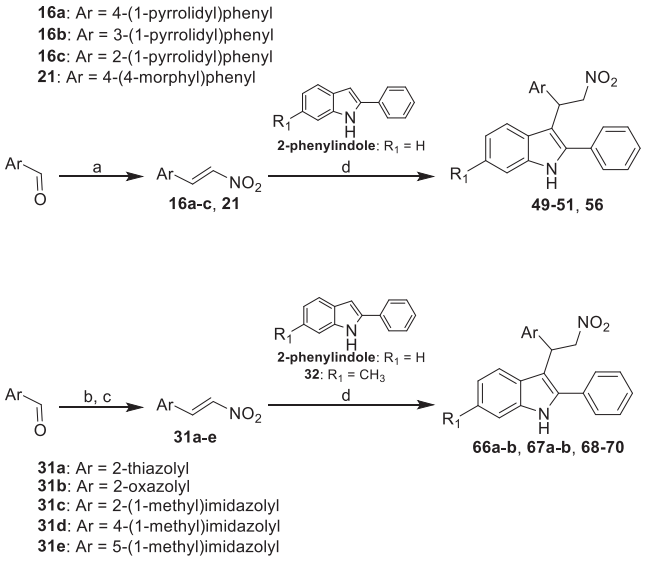

Scheme 1. Reagents and condition (a) NH_4 CF_3 CO_2 CH3NO2,reflux , 3–6 h; (b) XH_3NO_2,KO_t –Bu ,*t*-BuOH:THF,0°C,2–4;(c)Ac_2 O,4-DMAP, DCM,3–6 h;(d)NH_4 CF_3 CO_2 10%Aq. EtOH, reflux (100 °C,16 h) or microwave (120 °C, 30 min).

6-methylindole via oxidative 2-phenylation, was used as the nucleophile to generate the desired site-III analogs.[30] The syntheses of all other nitrovinyl BBs and site-III analogs not depicted in Scheme 1 are described in the Experimental section.

2.2. SAR studies: cAMP inhibition and β-arrestin recruitment

Focused on the GAT211 site-III phenyl ring, we first determined the impact of either extending or saturating the site-III phenyl ring on compound activity in a heterologous cell system expressing human CB1R (hCB1R). Functional profiling involved assay of cAMP production and β-arrestin recruitment. Since CB1R is canonically coupled to $G_{i/o}$, activation of CB1R inhibits cellular cAMP formation, and β-arrestin recruitment is a prime mode of G protein-independent CB1R signaling.[31] Ring extension by a single methylene unit decreased activity, as evidenced by benzyl analog **34** (Table 1), suggesting a one-carbon spacer between the 3-position of the indole ring and the site-III ring is optimal for activity. The cyclohexyl analog **35** also had less overall activity relative to GAT211 (**33**), demonstrating that an unsaturated site-III ring is preferred for activity, possibly as a reflection of its stabilizing electrostatic π-π interactions with aromatic CB1R residues. This proposition is supported by predictions from our previous, fragment-based docking analysis that the site-III phenyl ring of the GAT211 enantiomer, GAT228, forms a *T*-shape π-interaction with hCB1R F4.46 in the intracellular GPCR region and the site-III phenyl ring of the other enantiomer, GAT229, forms a parallel π-stack interaction with Y2.59 in the extracellular region.[28] These considerations focused our attention on an examination of the effects of site-III aromatic ring substituents in GAT211 analogs that retained the parent scaffold's single-carbon spacer between an unsaturated site-III phenyl-ring substituent and the 3-position of the indole ring.

GAT211 analogs monosubstituted at the *para*, *meta*, or *ortho* position on the site-III phenyl ring were synthesized and profiled. Within the methyl (**36–38**), methoxy (**39–41**), and chloro (**42–44**) series, the relative potency *ortho* > *meta* > *para* was observed, notably with respect to cAMP inhibition (Table 1). In the mono-fluoro series (**46–48**), the *para*-fluoro analog was a marginally more potent inhibitor of cAMP production than the *meta*-fluoro analog. The positive influence of lipophilicity at the site-III benzene ring *ortho* position on cAMP inhibition is evident from the much greater potency of the *ortho*-methyl (**38**) and *ortho*-chloro (**44**) analogs relative to GAT211 itself (**33**). However, this

Table 1

SAR data for site-III analogs in cAMP and β-arrestin assays[a-c].

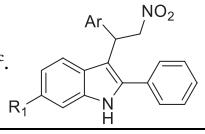

Compound	R_1	Ar	cAMP		β-Arrestin	
			EC_{50} (μM)	E_{Max} (% Response)	EC_{50} (μM)	E_{Max} (% Response)
33 GAT211	H	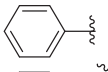	0.303	99.62	0.629	54.14
34	H	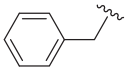	0.420	115.19	> 10	0
35	H	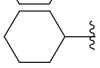	0.495	117.43	1.897	26.75
36	H	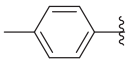	1.444	118.94	> 10	0
37	H	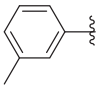	0.662	116.1	1.992	23.82
38	H	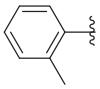	0.003	81.67	0.057	68.45
39	H	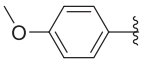	1.177	119.09	> 10	0
40	H	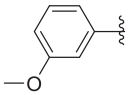	0.664	131.21	> 10	4.96
41	H	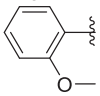	0.411	117.87	1.875	37.02
42	H	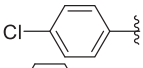	1.315	74.81	> 10	0
43	H	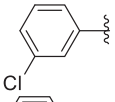	0.859	120.95	2.981	15.96
44	H	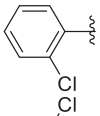	0.018	74.98	1.241	93.43
45	H	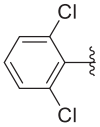	0.571	128.13	> 10	3.72
46	H	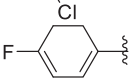	0.444	106.31	> 10	8.03
47	H	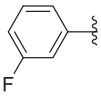	0.728	117.9	> 10	15.7
48	H	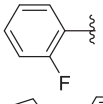	0.043	112.87	0.782	56.03
49	H	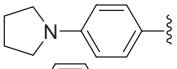	0.618	97.41	> 10	0
50	H	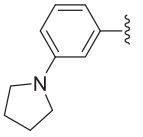	0.423	110.31	> 10	6.69

(*continued on next page*)

Table 1 (*continued*)

Compound	R_1	Ar	cAMP		β-Arrestin	
			EC_{50} (μM)	E_{Max} (% Response)	EC_{50} (μM)	E_{Max} (% Response)
51	H	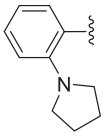	1.825	75.88	> 10	7.28
52	H	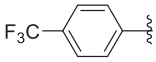	> 10	65.11	> 10	0
53	H	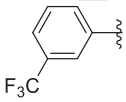	0.127	150.7	> 10	0
54	H	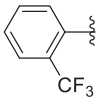	0.557	86.16	0.792	68.14
55	H	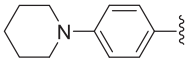	0.476	125.33	2.460	42.15
56	H	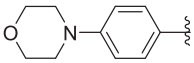	> 10	87.63	> 10	0
57	H	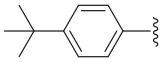	0.203	109.19	> 10	5.57
58	H	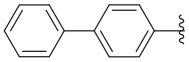	> 10	25.47	> 10	5
59	H	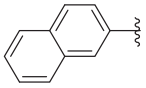	0.483	112.88	2.344	31.79
60	H	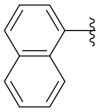	> 10	62.18	> 10	0
61	H		0.031	116.17	0.584	36.11
ZCZ011	CH_3		0.033	91.31	0.379	78.23
62	H		0.119	124.69	1.609	23.91
63	H		0.245	99.80	0.655	28.84
64	H		0.513	143.6	> 10	12.86
65	H		0.209	77.1	> 10	0.70
66a	H		0.192	83.65	0.331	32.59
66b	CH_3		0.050	98.45	0.163	80.62
67a	H		0.856	56.64	> 10	3.21
67b	CH_3		0.261	67.19	> 10	14.49
68	H	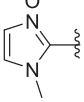	0.533	52.69	> 10	0
69	H	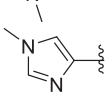	> 10	34.41	> 10	0.667

(*continued on next page*)

Table 1 (*continued*)

Compound	R_1	Ar	cAMP		β-Arrestin	
			EC_{50} (μM)	E_{Max} (% Response)	EC_{50} (μM)	E_{Max} (% Response)
70	H		> 10	46.06	> 10	0

[a]CB1R PAM activity was quantified for inhibition of forskolin-stimulated cellular cAMP production using the DiscoveRx HitHunter® assay (CHO hCB1R), EC_{20} of CP55,940, and test compound for 30 min, and for β-arrestin 2 recruitment using the DiscoveRx PathHunter® assay (CHO hCB1R) in cells treated with EC_{20} of CP55,940, and test compound for 90 min.

[b]n = 2–4 independent experiments were performed for each test concentration; 10 concentrations were examined over a 10,000-fold concentration range from 0.1 nM to 10 μM, and expressed as an average of these values (SD < ± 15%).

[c] A best-fit, dose-response curve was generated from data sets for each test compound using Chemical and Biological Information System (CBIS) data analysis suite.

influence appears to be limited since the 2,6-dichloro analog (**45**) was less potent as inhibitor of cAMP production than its monosubstituted version (**44**).

The potency trend *ortho* > *meta* > *para* for the monosubstituted GAT211 analogs was not entirely recapitulated in the 1-pyrrolidyl series (**49–51**) (Table 1**)**. As inhibitor of cellular cAMP production, the *meta*-pyrrolidyl analog (**50**) was indeed more potent than the *para* analog (**49**), whereas the *ortho*-1-pyrrolidinyl analog **51** was least potent. The pyrrolidyl-series SAR suggests that the bulky *ortho*- pyrrolidine ring might sterically hinder hCB1R-G protein interaction, thereby limiting the magnitude of downstream, $G_{\alpha i}$-mediated signaling. This suggestion is partially supported by the naphthyl-series SAR: the 2-naphthyl analog (**59**) was much more active in the cAMP assay than the 1-naphthyl analog (**60**). Within the trifluoromethyl series (**52–54**), the *meta*-substituted analog, **53**, provided the highest activity in cAMP inhibition; this finding might be attributed to a steric and/or electronic relationship. The pyrrolidyl- and naphthyl-series SARs, suggestive of a potential size limitation in the interior portion of the GAT211 site-III phenyl ring, led us to determine whether the *para*-position would be favorable for installing bulky substituents (**55–58**) (Table 1). The *para*-substituted 1-piperidyl GAT211 analog **55** was less active than parent **33** as inhibitor of cAMP production, and the *para*-substituted 4-morpholyl (**56**) and phenyl (**58**) analogs were entirely inactive. Among these *para*-substituted analogs, the *para-tert*-butyl compound **57** evidenced the highest potency in the cAMP assay.

These SAR data demonstrate that extended, 6-membered ring substituents with large surface areas are not well tolerated at the *para* position, regardless of their planarity or lipophilicity. Rather, the *para* position of the GAT211 scaffold preferentially accommodates compact, globular groups (e.g., **36, 39, 42, 46, 49, 57**).

We next transitioned our focus to site-III five-membered heteroaromatic ring substitutions. Notwithstanding the metabolic and toxicological liabilities of thiophene-containing drugs,[25,26] the 2-thienyl group is well tolerated at site III, as illustrated by ZCZ011 and ABD1236 (Figure 1). Alternative and more drug-like site-III five-membered heteroaromatic rings have not been intensively investigated. To this intent, we first wished to define the optimal heteroatom position within the ring. The SAR between 2 and *vs.* 3-thienyl (**61** *vs.* **62**) and 2- *vs.* 3-furyl (**63** *vs.* **64**) analogs in Table 1 demonstrates that placing the heteroatom at the 2-position yielded higher-potency compounds in the cAMP assay. It is noteworthy that the positional preference of the heteroatom within a five-membered aromatic ring is analogous to the *para* < *meta* < *ortho* trend exhibited by the methyl, chloro, and methoxy monosubstituted phenyl analogs. Among the thiophene and furan analogs, sulfur within site-III five-membered heteroaromatic rings yielded analogs with better overall activity in the cAMP assay than did oxygen as heteroatom (**61** *vs.* **63** and **62** *vs.* **64**).

These data led us to focus our site-III five-membered heteroaromatic SAR investigation on analogs with a heteroatom at the 2-position of the ring. The presence of nitrogen in the 2-pyrrolyl analog **65** marginally increased compound potency in the cAMP assay relative to furan analog **63**, but with reduced efficacy.

Considering the activity of **65** and the SARs around the thiophene (**61–62**) and furan (**63–64**) analogs, and the previous lack of knowledge on nitrogen's impact within a site-III five-membered heteroaromatic ring, we proceeded to install nitrogen into site-III sulfur- and oxygen-containing five-membered heteroaromatic rings with the intention of improving physiochemical properties while retaining biological activity. Accordingly, **61** was derivatized to the 2-thiazolyl analog **66a**, and **63** was derivatized to an oxazole, **67a**. In both instances, introducing nitrogen compromised activity in the cAMP assay (Table 1). Consistent with SAR for the thiophene and furan series, **66a** was more potent than **67a** in the cAMP assay, supporting the superiority of sulfur *vs.* oxygen within a five-membered site-III heteroaromatic ring.

Although SAR for the thiophene and furan series indicated that the 2-position is preferred for heteroatom localization, it remained unknown whether this positional preference could be extended to nitrogen-containing, five-membered heteroaromatic rings with two heteroatoms. To address this possibility experimentally, we synthesized and profiled three site-III *N*-methylimidazole analogs (**68–70**). As anticipated, the most potent *N*-methylimidazole analog in the cAMP assay, with activity comparable to that of **67a**, was the 2-substituted compound, **68**. The SAR across the thiophene, furan, and *N*-methylimidazole series allows conclusion that heteroatoms in the site-III five-membered rings positioned α- to the connecting tertiary carbon and facing toward the core of the 2-phenylindole scaffold foster excellent activity in the cAMP assay. This conclusion invites suggestion that methine groups at positions 3 and 4 of the site-III five-membered ring form key hydrophobic interactions with hCB1R residues that are critical for activity; replacement of these groups with hydrophilic oxygen or nitrogen heteroatoms could disrupt such important interactions. Mindful of this conclusion and our SAR data that support it, we nonetheless elected to examine experimentally the potential of nitrogen within a site-III five-membered heterocyclic ring to enhance compound aqueous solubility. Based on the structure of ZCZ011 and previously reported SAR studies,[20,22] we first modified the 2-thiazolyl analog **66a** and the 2-oxazolyl analog **67a** with the aim of improving potency by adding a methyl group in the 6-postion of the indole ring, yielding **66b** and **67b**, respectively (Table 1). A 6-methyl group increased potency in the cAMP assay by nearly four-fold, as demonstrated by comparing the activities of **66a** *vs.* **66b** and **67a** *vs.* **67b**. **66b** also showed robust activity in the β-arrestin recruitment assay not shared by **66a**, **67a,** and **67b,** implicating the site-III oxazole ring as a pharmacophore for potentially favoring G-protein-dependent signaling. Regarding inhibition of cAMP production, **67b** exhibited potency similar to GAT211. However, since limited aqueous solubility is characteristic of 2-phenylindole ago-PAMs, and aqueous solubility is an important drug-like characteristic, we reasoned from a therapeutic perspective that improved

Table 2
Kinetic water solubility of GAT211, ZCZ011, **66b**, and **67b**.

Compound	Solubility Limit (μM)
GAT211 (**33**)	1.56
ZCZ011	1.56
66b	3.13
67b	12.5

[a] Precipitation was determined by turbidity at 540 nm.
[b] Absorbance value > "mean +3 standard deviations" from blank was considered turbid.
[c] The coefficient of variation (CV) was < 1.5% for all four compounds.

aqueous solubility might counterbalance any potential potency reduction. The discovery of both **66b** and **67b** was highly encouraging, as they represent two analogs with the potential of possessing improved aqueous solubility with good biological activity.

2.3. Kinetic water solubility

Based upon the biological-activity and distinctive signaling profiles of **66b** and **67b**, we determined each of their kinetic water solubility using a standard turbidimetric assay in comparison to GAT211 and ZCZ011.

The aqueous solubilities of both **66b** and **67b** are improved over GAT211 and ZCZ011 (Table 2). Direct comparison of ZCZ011 and **66b** demonstrates that replacement of a site-III 2-thienyl for a 2-thiazolyl group improved kinetic water solubility by 2-fold without compromising their comparable *in vitro* activity in the cAMP assay. **67b** exhibited the best kinetic water solubility (8-fold greater than GAT211 and ZCZ011 and 4-fold greater than 66**b**), demonstrating that incorporation of a 2-oxazolyl moiety at site III is a tenable solution for improving the limited water solubility characteristic of the CB1R PAM 2-phenylindole scaffold.

3. Conclusions

Small-molecule PAMs are increasingly being recognized as potential pharmacotherapeutics that would leverage hCB1R as a drug target while avoiding the limitations of orthosteric CB1R agonists that have hindered their translation into the clinic.[15–18, 22], For this potential to be realized, extant libraries of biologically active CB1R PAMs need to be expanded from the standpoints of new chemical matter, SAR profiling, and drugability limitations. The present study addresses these considerations for a predominant class of CB1R PAMs, the 2-phenylindoles.[18,22] Syntheses and biological assessments of novel analogs derived from the 2-phenylindole scaffold reported here establish that the site-III functionality is a critical determinant of the biological activity of this class. Specifically, a site-III aromatic ring is necessary for appreciable CB1R ago-PAM activity. The hCB1R binding-pocket region for the site-III aromatic ring appears to have a rather strict size tolerance, as suggested by the compromise of biological activity elicited by extending GAT211′s site-III phenyl-ring or adding bulky substituents onto the ring itself. In contrast, introducing a small lipophilic group at the *ortho*-position of the GAT211 site-III phenyl ring (i.e., *o*-chloro or *o*-methyl) can significantly enhance hCB1R ago-PAM activity. The overall effect of a site-III *ortho* substituent, in terms of overall CB1R ago-PAM enhancement, may be attributed to the dihedral angle exerted by the substituent; this possibility will be inspected in future SAR studies. Aside from this *ortho* position for monosubstitution, the position *alpha* to the site-III ring's connecting tertiary carbon is the also amenable to modification without appreciably compromising bioactivity. While only marginally affecting biological activity, converting a site-III 2-thienyl to 2-thiazolyl moiety markedly increases compound water solubility, a finding that addresses one of the major physicochemical limitations of the of the 2-phenylindole class of CB1R PAMS. The comprehensive SAR data reported over a wide range of site-III aromatic ring variations on the 2-phenylindole scaffold provide ample context for candidate selection toward more detailed preclinical profiling, both *in vitro* for signaling bias[31,32] and *in vivo* for preclinical therapeutic efficacy. Enantiomeric separation of the most therapeutically promising site-III analogs will invite evaluation of the CB1R-related molecular pharmacology of each enantiomer. This initial SAR profiling should also be applicable to inform the design and optimization of next-generation 2-phenylindole CB1R ago-PAMs.

4. Experimental

4.1. Chemistry

4.1.1. Material and methods

All commercial reagents and solvents were purchased from Sigma Aldrich, Inc. (St. Louis, MO), Alfa Aesar (Ward Hill, MA), and Combi-Blocks (San Diego, CA) as reagent grade and used without further purification unless otherwise specified. A Biotage® Initiator Microwave System (Charlotte, NC) was used for synthesizing select intermediates. Reaction progress was monitored by thin-layer chromatography (TLC) using commercial silica gel 60 F254 glass plates. Compounds were visualized under ultraviolet light or by staining with iodine, phosphomolybdic acid, or *p*-anisaldehyde reagent. Flash column chromatography was carried out on a Biotage® SP1, Biotage® Isolera, or Interchim (Montluçon Cedex, France) purification unit using prepacked columns from Reveleris® (Buchi Corp., New Castle, DE), Biotage®, and Luknova (Boston, MA). Characterization of compounds and their purity were established by a combination of HPLC, TLC, mass spectrometry, and NMR analyses. NMR spectra were recorded in DMSO-d_6, chloroform-d, or methanol-d_4, on a Varian NMR spectrometer (1H NMR at 500 MHz and 13C NMR at 125 MHz) (Agilent Technologies, Palo Alto, CA). Chemical shifts were recorded in parts per million (δ) relative to tetramethylsilane (TMS; 0.00 ppm) or solvent peaks as the internal reference. Multiplicities are indicated as br (broadened), s (singlet), d (doublet), t (triplet), q (quartet), quin (quintet), sept (septet), or m (multiplet). Coupling constants (J) are reported in hertz (Hz). All test compounds were > 95% pure as determined by LC/MS analysis performed using an Agilent Technologies 1260 Infinity reverse phase HPLC with dual-wavelength UV–visible detector and a 6120 Quadrupole mass spectrometer (electrospray ionization). HRMS was done on SCIEX TOF/TOF™ 5800 System (Framingham, MA) in a positive-ion mode with delay time of 100 ns. Each sample well was surveyed to find a "sweet spot", and 400 laser pulses were then averaged to generate a spectrum.

4.1.2.-4.1.16. **1–15**

The following intermediates were prepared by previously reported general procedures: ***1***;[33] ***5***; [34,35] ***2–3***, ***8***;[36] ***4–7***, ***9–10***;[37] ***11***;[38] ***12***; [39] ***13–15***. [24]

4.1.2. General Procedure A: Syntheses of pyrrolidyl-substituted phenyl nitrovinyl intermediates (16a-16c)

To a 100-mL round bottom flask was added pyrrolidyl-benzaldehyde (460 mg, 2.63 mmol, 1 eq.), ammonium trifluoroacetate (202 mg, 2.63 mmol, 1 eq.), and nitromethane (40 mL). The reaction mixture was refluxed under argon for 3–6 h. Upon reaction completion, the reaction mixture was cooled to room temperature, concentrated under reduced pressure, diluted with dichloromethane, then washed with ice-cold water. The aqueous phase was extracted 3X with dichloromethane. Combined organic extracts were washed with brine, dried with sodium sulfate, then concentrated under reduced pressure. The resulting organic resin was purified by silica gel flash chromatography using ethyl acetate/hexanes eluent to afford the pure nitrovinyl product.

4.1.2.1. (EV)-1-(4-(2-nitrovinyl)phenyl)pyrrolidine ***(16a)***. Yield: 40%; ^{1}H NMR (500 MHz, ($CDCl_3$): δ 7.96 (d, J = 13.5 Hz, 1H), 7.48 (d,

J = 13.0 Hz, 1H), 7.41 (d, J = 8.5 Hz, 2H), 7.41 (d, J = 9.0 Hz, 2H), 3.39–3.36 (m, 4H), 2.07–2.04 (m, 4H).

*4.1.2.2. (E)-1-(3-(2-nitrovinyl)phenyl)pyrrolidine (**16b**)*. Yield: 77%; ^{1}H NMR (500 MHz, $CDCl_3$): δ 7.95 (d, J = 13.5 Hz, 1H), 7.57 (d, J = 14.0 Hz, 1H), 7.27 (t, J = 4.5 Hz, 1H), 6.83 (d, J = 7.5 Hz, 1H), 6.68 (dd, J = 8.0 Hz, J = 4.0 Hz, 1H), 6.63 (t, J = 4.0 Hz, 1H), 3.33–3.29 (m, 4H), 2.06–2.02 (m, 4H).

*4.1.2.3. (E)-1-(2-(2-nitrovinyl)phenyl)pyrrolidine (**16c**)*. Yield: 87%. NMR was confirmed by referring to the corresponding previously reported spectrum.[40]

4.1.18.-4.1.21. **17–20**

The following intermediates were prepared by previously reported general procedures: ***17–18***; [41] ***19***; [42] ***20***. [19]

*4.1.3. (E)-4-(4-(2-nitrovinyl)phenyl)morpholine (**21**)*

The intermediate was prepared from 4-morpholinobenzaldehyde using General Procedure A. Yield: 44%; ^{1}H NMR (500 MHz, $(CD_3)_2SO$): δ 8.06 (d, J = 13.5 Hz, 1H), 8.03 (d, J = 13.5 Hz, 1H), 7.20 (d, J = 9.0 Hz, 2H), 7.00 (d, J = 8.0 Hz, 2H), 3.74–3.71 (m, 4H), 3.34–3.30 (m, 4H).

4.1.22.-4.1.30. **22–30**

The following intermediates were prepared by previously reported general procedures: ***22***; [43] ***23–24***; [37] ***25***; [39] ***26***; [36] ***27***; [44,45] ***28***; [19] ***29***; [46] ***30***. [47]

*4.1.4. General Procedure B: Two-step syntheses of thiazole, oxazole, and N-methylimidazole nitrovinyl intermediates (**31a-31e**)*

Procedures used for both steps were derived from a previously reported method.[29]

To a solution of aromatic aldehyde (5.3 mmol, 1 eq.) in tBuOH:THF (1:1; 6 mL) was added nitromethane (8.48 mmol, 1.6 eq.). The reaction mixture was stirred at 0 °C, then potassium *tert*-butoxide (0.32 mmol, 6 mol%) was added directly. Following 2–5 h of stirring at 0 °C, the reaction mixture was concentrated under reduced pressure to remove tBuOH, diluted with ethyl acetate, then washed with water and brine. The aqueous phase was extracted 3X with ethyl acetate, and the combined organic extracts were dried with sodium sulfate, then concentrated under reduced pressure. The nitroalcohol intermediate obtained from workup was used for the next step without further purification.

To a 100-mL round bottom flask containing the nitroalcohol intermediate (4.25 mmol, 1 eq.) and 4-DMAP (0.21 mmol, 5 mol%) was added anhydrous dichloromethane (20 mL). The mixture was stirred under argon at room temp. Acetic anhydride (4.68 mmol, 1.1 eq.) was added dropwise to the stirring mixture, and the resulting reaction mixture continued stirring under argon at room temperature. Following 2–5 h of room-temperature stirring, the reaction mixture was quenched with saturated $NaHCO_3$ solution, then washed with water and brine. The aqueous phase was extracted 3X with dichloromethane, and the combined organic extracts were dried with sodium sulfate, then concentrated under reduced pressure. The crude organic resin was purified by silica gel flash chromatography using ethyl acetate/hexanes eluent to obtain the desired nitrovinyl product.

*4.1.4.1. (E)-2-(2-nitrovinyl)thiazole (**31a**)*. Yield: 58%; ^{1}H NMR (500 MHz, $CDCl_3$) δ: 8.07 (d, J = 13.4 Hz, 1H), 8.05 (d, J = 3.1 Hz, 1H), 7.90 (d, J = 13.4 Hz, 1H), 7.64 (d, J = 3.1 Hz, 1H).

*4.1.4.2. (E)-2-(2-nitrovinyl)oxazole (**31b**)*. Yield: 32%; ^{1}H NMR (500 MHz, $CDCl_3$) δ: 7.84 – 7.77 (m, 3H), 7.40 (s, 1H).

*4.1.4.3. (E)-1-methyl-2-(2-nitrovinyl)-1H-imidazole (**31c**)*. Yield: 32%; ^{1}H NMR (500 MHz, $CDCl_3$) δ: 7.92 (d, J = 12.9 Hz, 1H), 7.84 (d, J = 13.0 Hz, 1H), 7.26 – 7.24 (m, 1H), 7.14 – 7.10 (m, 1H), 3.83 (s, 3H).

*4.1.4.4. (E)-1-methyl-4-(2-nitrovinyl)-1H-imidazole (**31d**)*. Yield: 55%; ^{1}H NMR (500 MHz, $CDCl_3$) δ 7.86 (d, J = 13.1 Hz, 1H), 7.76 (d, J = 13.1 Hz, 1H), 7.52 (s, 1H), 7.28 (s, 1H), 3.75 (s, 3H).

4.1.4.5. (E)-1-methyl-5-(2-nitrovinyl)-1H-imidazole (31e). Yield: 60%; ^{1}H NMR (500 MHz, $CDCl_3$) δ: 7.94 (d, J = 13.6 Hz, 1H), 7.67 (s, 1H), 7.63 (s, 1H), 7.53 (d, J = 13.6 Hz, 1H), 3.80 (s, 3H).

*4.1.5. General Procedure C: Synthesis of 6-methyl-2-phenylindole (**32**)*

Procedures were previously reported method.[30]

To a 100-mL round bottom flask was added 6-methylindole (1 g, 7.62 mmol, 1 eq.), phenylboronic acid (1.858 g, 15.24 mmol, 2 eq.), palladium (ii) acetate (86 mg, 0.381 mmol, 5 mol%), and acetic acid (12 mL). The atmosphere within the reaction flask was evacuated under vacuum, then backfilled with oxygen gas. Oxygen flushing was conducted 4X. The reaction mixture was stirred at room temperature under moderately high pressure of oxygen gas for 23 h. Following reaction completion, the mixture was concentrated under reduced pressure, diluted with ethyl acetate, then filtered through a celite pad. Collected filtrate was concentrated under reduced pressure, and the resulting organic resin was purified by silica gel flash chromatography using ethyl acetate/hexanes eluent to yield the desired product. Yield: 68%

*4.1.6. General Procedure D: C3 alkylation of 2-phenylindoles with nitrovinyl intermediates (**33–70**)*

To a 100-mL round bottom flask containing 2-phenyl-1H-indole (1.0 mmol, 1 eq.), nitrovinyl building block (1.5 mmol, 1.5 eq.) and CF_3COONH_4 (0.5 mmol) were dissolved with 10% aq. EtOH (10 mL). The reaction mixture was refluxed at 105 °C for 12–18 h. After reaction completion, the mixture was concentrated under reduced pressure to remove EtOH, diluted with ethyl acetate, then washed with water and brine. The aqueous phase was extracted 3X with ethyl acetate, and the combined organic extracts were dried with Na_2SO_4 then concentrated under reduced pressure. The crude organic resin was purified by silica gel flash chromatography using ethyl acetate/hexanes eluent to obtain the desired conjugate product.

*4.1.6.1. 3-(2-nitro-1-phenylethyl)-2-phenyl-1H-indole (**33**)*. The final compound was prepared using commercially available 2-phenylindole and β-nitrostyrene. Yield: 92%. NMR was previously reported.[19]

*4.1.6.2. 3-(1-nitro-3-phenylpropan-2-yl)-2-phenyl-1H-indole (**34**)*. The final compound was prepared using commercially available 2-phenylindole and **1**. Yield: 52%; ^{1}H NMR (500 MHz, $CDCl_3$): δ 7.96 (s, 1H), 7.76 (d, J = 7.5 Hz, 1H), 7.39 (d, J = 8.0 Hz, 1H), 7.35–7.30 (m, 3H), 7.25 (td, J = 7.0, 1.0 Hz, 1H), 7.21 (td, J = 7.0, 1.0 Hz, 1H), 7.14–7.10 (m, 3H), 6.97 (dd, J = 8.0, 2.0 Hz, 2H), 6.89 (dd, J = 8.0, 2.0 Hz, 2H), 4.90–4.81 (m,2H), 4.09–4.03 (m, 1H), 3.31 (dd, J = 13.5, 10.0 Hz, 1H), 3.09 (dd, J = 13.5, 10.0 Hz, 1H).

4.1.6.3. 3-(1-cyclohexyl-2-nitroethyl)-2-phenyl-1H-indole (35). The final compound was prepared using commercially available 2-phenylindole and **2**. Yield: 72%; ^{1}H NMR (500 MHz, $CDCl_3$): δ 8.02 (s, 1H), 7.63 (d, J = 8.0 Hz, 1H), 7.50–7.42 (m, 5H), 7.37 (d, J = 8.0 Hz, 1H), 7.21 (t, J = 7.5 Hz, 2H), 7.14 (t, J = 7.5 Hz, 2H), 4.96–4.86 (m, 2H), 3.66–3.61 (m, 1H), 1.96–1.88 (m, 1H), 1.83–1.72 (m, 2H), 1.59–1.47 (m, 4H), 1.27–1.18 (m, 1H), 1.11–1.04 (m, 3H), 0.79–0.71 (m, 1H). HRMS Calcd for $C_{22}H_{24}N_2O_2$ $[M]^+$ 348.1838, found 348.1836

4.1.6.4. 3-(2-nitro-1-(p-tolyl)ethyl)-2-phenyl-1H-indole (36). The final compound was prepared using commercially available 2-phenylindole and **3**. Yield: 85%; ^{1}H NMR (500 MHz, $CDCl_3$): δ 8.15 (s, 1H), 7.52 (d, J = 7.5 Hz, 1H), 7.47–7.42 (m, 5H), 7.39 (d, J = 7.5 Hz, 1H), 7.25–7.19 (m, 3H), 7.12–7.09 (m, 3H), 5.27 (t, J = 8.5 Hz, 1H),

5.18–5.09 (m, 2H), 2.30 (s, 3H). HRMS Calcd for $C_{23}H_{20}N_2O_2$ $[M]^+$ 356.1525, found 356.1552

4.1.6.5. 3-(2-nitro-1-(m-tolyl)ethyl)-2-phenyl-1H-indole (37). The final compound was prepared using commercially available 2-phenylindole and **4**. Yield: 88%; ^{1}H NMR (500 MHz, $CDCl_3$): δ 8.18 (s, 1H), 7.58 (d, J = 8.0 Hz, 1H), 7.49–7.46 (m, 5H), 7.25 (t, J = 7.5 Hz, 1H), 7.21 (t, J = 7.0 Hz, 1H), 7.18–7.13 (m, 3H), 7.08 (d, J = 7.5 Hz, 1H), 5.33 (t, J = 7.5 Hz, 1H), 5.22–5.13 (m, 2H). HRMS Calcd for $C_{23}H_{20}N_2O_2$ $[M]^+$ 356.1525, found 356.1533

4.1.6.6. 3-(2-nitro-1-(o-tolyl)ethyl)-2-phenyl-1H-indoleindole (38). The final compound was prepared using commercially available 2-phenylindole and **5**. Yield: 74%; ^{1}H NMR (500 MHz, $CDCl_3$): δ 8.13 (s, 1H), 7.66 (d, J = 8.0 Hz, 1H), 7.52 (d, J = 8.0 Hz, 1H), 7.47–7.42 (m, 3H), 7.38–7.36 (m, 3H), 7.21 (t, J = 7.5 Hz, 1H), 7.14–7.11 (m, 4H), 5.42 (t, J = 8.0 Hz, 1H), 5.19 (dd, J = 13.5, 8.5 Hz, 1H), 5.06 (dd, J = 13.5, 8.5 Hz, 1H), 2.14 (s, 3H). HRMS Calcd for $C_{23}H_{20}N_2O_2$ $[M]^+$ 356.1525, found 356.1514

4.1.6.7. 3-(1-(4-methoxyphenyl)-2-nitroethyl)-2-phenyl-1H-indole (39). The final compound was prepared using commercially available 2-phenylindole and **6**. Yield: 86%; ^{1}H NMR (500 MHz, $CDCl_3$): δ 8.14 (s, 1H), 7.54 (d, J = 8.0 Hz, 1H), 7.48–7.39 (m, 6H), 7.27–7.20 (m, 3H), 7.12 (dd, J = 7.5, 1.0 Hz, 1H), 6.83 (dt, J = 8.5, 3.5 Hz, 2H), 5.26 (t, J = 8.0 Hz, 1H), 5.17–5.07 (m, 2H), 3.77 (s, 3H). HRMS Calcd for $C_{23}H_{20}N_2O_3$ $[M]^+$ 372.1474, found 374.1487

4.1.6.8. 3-(1-(3-methoxyphenyl)-2-nitroethyl)-2-phenyl-1H-indole (40). The final compound was prepared using commercially available 2-phenylindole and **7**. Yield: 81%; ^{1}H NMR (500 MHz, $CDCl_3$): δ 8.16 (s, 1H), 7.55 (d, J = 8.0 Hz, 1H), 7.45–7.39 (m, 5H), 7.36 (d, J = 8.0 Hz, 1H), 7.24–7.18 (m, 2H), 7.11 (t, J = 8.0 Hz, 1H), 6.92 (dd, J = 8.0, 2.0 Hz, 1H), 6.87 (t, J = 2.0 Hz, 1H), 6.76 (dd, J = 8.5, 2.5 Hz, 1H), 5.28 (t, J = 8.0 Hz, 1H), 5.18–5.09 (m, 2H), 3.71 (s, 3H). HRMS Calcd for $C_{23}H_{20}N_2O_3$ $[M]^+$ 372.1474, found 374.1461

4.1.6.9. 3-(1-(2-methoxyphenyl)-2-nitroethyl)-2-phenyl-1H-indole (41). The final compound was prepared using commercially available 2-phenylindole and **8**. Yield: 87%; ^{1}H NMR (500 MHz, $CDCl_3$): δ 8.13 (s, 1H), 7.65 (d, J = 7.5 Hz, 1H), 7.45–7.34 (m, 7H), 7.26–7.20 (m, 2H), 7.13 (t, J = 8.0 Hz, 1H), 6.89 (d, J = 7.5 Hz, 1H), 6.84 (t, J = 8.0 Hz, 1H), 5.6 (dd, J = 6.5, 2.5 Hz, 1H), 5.18–5.14 (m, 2H), 3.77 (s, 3H). HRMS Calcd for $C_{23}H_{20}N_2O_3$ $[M]^+$ 372.1474, found 374.1497

4.1.6.10. 3-(1-(4-chlorophenyl)-2-nitroethyl)-2-phenyl-1H-indole (42). The final compound was prepared using commercially available 2-phenylindole and **9**. Yield: 82%; ^{1}H NMR (500 MHz, $CDCl_3$): δ 8.17 (s, 1H), 7.49–7.39 (m, 7H), 7.27–7.25 (m, 4H), 7.23 (dd, J = 7.5, 1.0 Hz, 1H), 7.12 (dd, J = 7.5, 1.0 Hz, 1H), 5.28 (t, J = 8.0 Hz, 1H), 5.16 (dd, J = 12.0, 7.0 Hz, 1H), 5.09 (dd, J = 13.5, 10.5 Hz, 1H). HRMS Calcd for $C_{22}H_{17}ClN_2O_2$ $[M]^+$ 376.0979, found 376.0906

4.1.6.11. 3-(1-(3-chlorophenyl)-2-nitroethyl)-2-phenyl-1H-indole (43). The final compound was prepared using commercially available 2-phenylindole and **10**. Yield: 84%;^{1}H NMR (500 MHz, $CDCl_3$): δ 8.15 (s, 1H), 7.48 (d, J = 7.5 Hz, 1H), 7.46–7.37 (m, 5H), 7.35 (d, J = 7.54 Hz, 1H), 7.28 (s, 1H), 7.21–7.18 (m, 4H), 7.11 (dd, J = 7.5, 1.0 Hz, 1H), 5.27 (t, J = 8.0 Hz, 1H), 5.15–5.04 (m, 2H). HRMS Calcd for $C_{22}H_{17}ClN_2O_2$ $[M]^+$ 376.0979, found 376.0992

4.1.6.12. 3-(1-(2-chlorophenyl)-2-nitroethyl)-2-phenyl-1H-indole (44). The final compound was prepared using commercially available 2-phenylindole and **11**. Yield: 73%; ^{1}H NMR (500 MHz, $CDCl_3$): δ 8.20 (s, 1H), 7.69 (d, J = 8.0 Hz, 1H), 7.59 (d, J = 8.0 Hz, 1H), 7.46–7.36 (m, 7H), 7.26–7.16 (m, 4H), 5.68 (dd, J = 10.0, 6.0 Hz, 1H), 5.23 (dd, J = 13.5, 10.5 Hz, 1H), 5.08 (dd, J = 10.0 Hz, 6.0 Hz, 1H). HRMS Calcd for $C_{22}H_{17}ClN_2O_2$ $[M]^+$ 376.0979, found 376.0988

4.1.6.13. 3-(1-(2,6-dichlorophenyl)-2-nitroethyl)-2-phenyl-1H-indole (45). The final compound was prepared using commercially available 2-phenylindole and **12**. Yield: 86%; ^{1}H NMR (500 MHz, $CDCl_3$): δ 7.99 (s, 1H), 7.38–7.27 (m, 7H), 7.18–7.14 (m, 3H), 7.06–7.01 (m, 2H), 5.15 (dd, J = 8.5, 7.0 Hz, 1H), 5.29–5.21 (m, 2H). HRMS Calcd for $C_{22}H_{16}Cl_2N_2O_2$ $[M]^+$ 410.0589, found 410.0555

4.1.6.14. 3-(1-(4-fluorophenyl)-2-nitroethyl)-2-phenyl-1H-indole (46). The final compound was prepared using commercially available 2-phenyl indole and **13**. NMR was previously reported.[24]

4.1.6.15. 3-(1-(3-fluorophenyl)-2-nitroethyl)-2-phenyl-1H-indole (47). The final compound was prepared using commercially available 2-phenyl indole and **14**. NMR was previously reported.[24]

4.1.6.16. 3-(1-(2-fluorophenyl)-2-nitroethyl)-2-phenyl-1H-indole (48). The final compound was prepared using commercially available 2-phenyl indole and **15**. NMR was previously reported.[24]

4.1.6.17. 3-(2-nitro-1-(4-(pyrrolidin-1-yl)phenyl)ethyl)-2-phenyl-1H-indole (49). The final compound was prepared using commercially available 2-phenylindole and **16a**. Yield: 72%; ^{1}H NMR (500 MHz, $CDCl_3$): δ 8.07 (s, 1H), 7.58 (d, J = 8.0 Hz, 1H), 7.43–7.37 (m, 5H), 7.34 (d, J = 8.0 Hz, 1H), 7.20–7.16 (m, 3H), 7.09 (t, J = 8.0 Hz, 1H), 6.48–6.45 (m, 2H), 5.20 (t, J = 8.5 Hz, 1H), 5.11–5.05 (m, 2H), 3.23–3.20 (m, 4H), 1.96–1.93 (m, 4H). HRMS Calcd for $C_{26}H_{25}N_3O_2$ $[M]^+$ 411.1947, found 411.1916

4.1.6.18. 3-(2-nitro-1-(3-(pyrrolidin-1-yl)phenyl)ethyl)-2-phenyl-1H-indole (50). The final compound was prepared using commercially available 2-phenylindole and **16b**. Yield: 70%; ^{1}H NMR (500 MHz, $CDCl_3$): δ 8.11 (s, 1H), 7.64 (d, J = 8.1 Hz, 1H), 7.50 – 7.38 (m, 5H), 7.36 (d, J = 8.1 Hz, 1H), 7.22 – 7.17 (m, 1H), 7.16 – 7.09 (m, 2H), 6.64 (d, J = 7.7 Hz, 1H), 6.54 (s, 1H), 6.44 (d, J = 8.2 Hz, 1H), 5.24 (t, J = 7.9 Hz, 1H), 5.20 – 5.10 (m, 2H), 3.22 – 3.12 (m, 4H), 1.98 – 1.90 (m, 4H). HRMS Calcd for $C_{26}H_{25}N_3O_2$ $[M]^+$ 411.1947, found 411.1936

4.1.6.19. 3-(2-nitro-1-(2-(pyrrolidin-1-yl)phenyl)ethyl)-2-phenyl-1H-indole (51). The final compound was prepared using commercially available 2-phenylindole and **16c**. ^{1}H NMR (500 MHz, $CDCl_3$): δ 8.20 (s, 1H), 7.58 (d, J = 8.0 Hz, 1H), 7.46 – 7.37 (m, 6H), 7.35 (dd, J = 7.8, 1.5 Hz, 1H), 7.26 – 7.17 (m, 3H), 7.13 (t, J = 7.6 Hz, 1H), 6.89 (td, J = 7.5, 1.5 Hz, 1H), 5.65 (dd, J = 10.6, 4.5 Hz, 1H), 5.42 (dd, J = 12.6, 4.5 Hz, 1H), 5.11 (dd, J = 12.7, 10.6 Hz, 1H), 3.36 – 3.27 (m, 2H), 2.92 – 2.84 (m, 2H), 1.95 – 1.86 (m, 2H), 1.86 – 1.75 (m, 2H). Yield: 47%; HRMS Calcd for $C_{26}H_{25}N_3O_2$ $[M]^+$ 411.1947, found 411.1908

4.1.6.20. 3-(2-nitro-1-(4-(trifluoromethyl)phenyl)ethyl)-2-phenyl-1H-indole (52). The final compound was prepared using commercially available 2-phenylindole and **17**. Yield: 84%; ^{1}H NMR (500 MHz, $CDCl_3$): δ 8.20 (s, 1H), 7.56 (s, 1H), 7.54 (s, 1H), 7.50–7.41 (m, 9H), 7.24 (t, J = 7.5 Hz, 1H), 7.14 (t, J = 7.0 Hz, 1H), 5.37 (t, J = 8.0 Hz, 1H), 5.22 (dd, J = 12.5, 7.5 Hz, 1H), 5.13 (dd, J = 12.5, 7.5 Hz, 1H). HRMS Calcd for $C_{22}H_{17}F_3N_2O_2$ $[M]^+$ 410.1242, found 410.1284

4.1.6.21. 3-(2-nitro-1-(3-(trifluoromethyl)phenyl)ethyl)-2-phenyl-1H-indole (53). The final compound was prepared using commercially available 2-phenylindole and **18**. Yield: 80%; ^{1}H NMR (500 MHz, $CDCl_3$): δ 8.15 (s, 1H), 7.56 (s, 1H), 7.48 (t, J = 8.0 Hz, 3H), 7.45–7.41 (m, 3H), 7.37–7.34 (m, 4H), 7.20 (t, J = 8.0 Hz, 1H), 7.12 (t, J = 8.0 Hz, 1H), 5.34 (t, J = 7.5 Hz, 1H), 5.18–5.08 (m, 2H).). HRMS Calcd for $C_{23}H_{17}F_3N_2O_2$ $[M]^+$ 410.1242, found 410.1246

4.1.6.22. 3-(2-nitro-1-(2-(trifluoromethyl)phenyl)ethyl)-2-phenyl-1H-indole (54). The final compound was prepared using commercially available 2-phenylindole and **19**. Yield: 84%; ^{1}H NMR (500 MHz, $CDCl_3$): δ 8.16 (s, 1H), 7.84 (d, J = 8.0 Hz, 1H), 7.76 (d, J = 8.0 Hz, 1H), 7.67 (dd, J = 7.5, 1.0 Hz, 1H), 7.43–7.34 (m, 7H), 7.27–7.23 (m, 2H), 7.21 (td, J = 7.5, 1.5 Hz, 1H), 5.76 (dd, J = 10.0, 4.5 Hz, 1H), 5.34 (dd, J = 13.5, 10.5 Hz, 1H), 4.90 (dd, J = 13.5, 6.0 Hz, 1H) HRMS Calcd for $C_{23}H_{17}F_3N_2O_2$ $[M]^+$ 410.1242, found 410.1211

4.1.6.23. 3-(2-nitro-1-(4-(piperidin-1-yl)phenyl)ethyl)-2-phenyl-1H-indole (55). The final compound was prepared using commercially available 2-phenylindole and **20**. Yield: 77%; ^{1}H NMR (500 MHz, $CDCl_3$): δ 8.14 (s, 1H), 7.54 (d, J = 7.5 Hz, 1H), 7.46–7.39 (m, 5H), 7.38 (d, J = 8.0 Hz, 1H), 7.23–7.18 (m, 3H), 7.11 (t, J = 7.5 Hz, 1H), 6.84 (d, J = 9.0 Hz, 2H), 5.23 (t, J = 8.0 Hz, 1H), 5.15–5.07 (m, 2H), 3.11 (t, J = 5.5 Hz, 4H), 1.71–1.64 (m , 4H), 1.58–1.52 (m, 2H). HRMS Calcd for $C_{27}H_{27}N_3O_2$ $[M]^+$ 425.2103, found 425.2126

4.1.6.24. 4-(4-(2-nitro-1-(2-phenyl-1H-indol-3-yl)ethyl)phenyl) morpholine (56). The final compound was prepared using commercially available 2-phenylindole and **21**. Yield: 67%; ^{1}H NMR (500 MHz, $CDCl_3$): δ 8.18 (s, 1H), 7.53 (dd, J = 8.0, 2.5 Hz, 1H), 7.50 – 7.37 (m, 6H), 7.25 – 7.19 (m, 3H), 7.11 (td, J = 7.8, 2.4 Hz, 1H), 6.92 – 6.81 (m, 2H), 5.28 – 5.22 (m, 1H), 5.18 – 5.06 (m, 2H), 3.91 – 3.79 (m, 4H), 3.18 – 3.09 (m, 4H). HRMS Calcd for $C_{26}H_{26}N_3O_3$ $[M+H]^+$ 428.1916, found 428.1951

4.1.6.25. 3-(1-(4-(tert-butyl)phenyl)-2-nitroethyl)-2-phenyl-1H-indole (57). The final compound was prepared using commercially available 2-phenylindole and **22**. Yield: 81%; ^{1}H NMR (500 MHz, $CDCl_3$): δ 8.13 (s, 1H), 7.56 (d, J = 7.0 Hz, 1H), 7.46–7.38 (m, 6H), 7.30 (dt, J = 8.0, 2.0 Hz, 2H), 7.26 (d, J = 7.0 Hz, 2H), 7.21 (td, J = 7.5, 1.5 Hz, 1H), 7.12 (td, J = 8.0, 1.0 Hz, 1H), 5.29 (d, J = 7.0 Hz, 1H), 5.19–5.11 (m, 2H), 1.28 (s, 9H). HRMS Calcd for $C_{26}H_{26}N_2O_2$ $[M]^+$ 398.1994, found 398.1972

4.1.6.26. 3-(1-([1,1′-biphenyl]-4-yl)-2-nitroethyl)-2-phenyl-1H-indole (58). The final compound was prepared using commercially available 2-phenylindole and **23**. Yield: 71%; ^{1}H NMR (500 MHz, $CDCl_3$): δ 8.18 (s, 1H), 7.59–7.51 (m, 5H), 7.50–7.39 (m, 10*H*), 7.33 (tt, J = 7.5, 1.5 Hz, 1H), 7.24 (t, J = 8.0 Hz, 1H), 7.14 (t, J = 8.0 Hz, 1H), 5.37 (t, J = 8.0 Hz, 1H), 5.23 (dd, J = 12.0, 7.5 Hz, 1H), 5.17 (dd, J = 13.0, 8.0 Hz, 1H). HRMS Calcd for $C_{28}H_{22}N_2O_2$ $[M]^+$ 418.1681, found 418.1693

4.1.6.27. 3-(1-(naphthalen-2-yl)-2-nitroethyl)-2-phenyl-1H-indole (59). The final compound was prepared using commercially available 2-phenylindole and **24**. Yield: 76%; ^{1}H NMR (500 MHz, $CDCl_3$): δ 8.17 (bs, 1H), 7.97(d, J = 8.5 Hz, 1H), 7.87 (d, J = 8.5 Hz, 1H), 7.76–7.69 (m, 3H), 7.48–7.32 (m, 8H), 7.23 (t, J = 7.5, 1.0 Hz, 2H), 7.17(t, J = 7.5, 1.0 Hz, 1H), 6.06 (dd, J = 9.0, 6.0 Hz, 1H), 5.35 (dd, J = 13.0, 9.5 Hz, 1H), 5.20 (dd, J = 12.5, 6.0 Hz, 1H). HRMS Calcd for $C_{26}H_{20}N_2O_2$ $[M]^+$ 392.1525, found 392.1511

4.1.6.28. 3-(1-(naphthalen-1-yl)-2-nitroethyl)-2-phenyl-1H-indole (60). The final compound was prepared using commercially available 2-phenylindole and **25**. Yield: 72%; ^{1}H NMR (500 MHz, $CDCl_3$): δ 8.20 (s, 1H), 7.81–7.74 (m, 4H), 7.56 (d, J = 8.0 Hz, 1H), 7.49–7.41 (m, 9H), 7.23 (t, J = 8.0, 1.0 Hz, 1H), 7.11 (t, J = 8.0, 1.0 Hz, 1H), 5.48 (t, J = 8.0 Hz, 1H), 5.32 (dd, J = 13.0, 7.5 Hz, 1H), 5.22 (dd, J = 13.0, 8.0 Hz, 1H). HRMS Calcd for $C_{26}H_{20}N_2O_2$ $[M]^+$ 392.1525, found 392.1559

4.1.6.29. 3-(2-nitro-1-(thiophen-2-yl)ethyl)-2-phenyl-1H-indole (61). The final compound was prepared using commercially available 2-phenylindole and **26**. Yield: 82%; ^{1}H NMR (500 MHz, $CDCl_3$): δ 8.14 (s, 1H), 7.52 (d, J = 8.0 Hz, 1H), 7.49–7.41 (m, 5H), 7.38 (d, J = 8.0 Hz, 1H), 7.23 (dd, J = 5.0, 1.0 Hz, 1H), 7.19 (dd, , J = 5.0, 1.0 Hz, 1H), 7.11 (t, J = 8.0 Hz, 1H), 6.92 (d, J = 5.0 Hz, 2H), 5.49 (t, J = 8.5 Hz, 1H), 5.18 (dd, J = 12.5, 7.5 Hz, 1H), 5.08 (dd, J = 12.5, 8.0 Hz, 1H). HRMS Calcd for $C_{20}H_{16}N_2O_2S$ $[M]^+$ 348.0932, found 348.0958

4.1.6.30. 3-(2-nitro-1-(thiophen-3-yl)ethyl)-2-phenyl-1H-indole (62). The final compound was prepared using commercially available 2-phenylindole and **27**. Yield: 80%; ^{1}H NMR ($CDCl_3$, 500 MHz): δ 8.11 (s, 1H), 7.46–7.39 (m, 6H), 7.37 (d, J = 8.5 Hz, 1H), 7.24 (t, J = 5.0 Hz, 1H), 7.20 (td, J = 7.0 Hz, 1.0 Hz, 1H), 7.11–7.07 (m, 2H), 6.95 (dd, J = 5.0, 1.0 Hz, 1H), 5.32 (t, J = 8.0 Hz, 1H), 5.15 (dd, J = 12.5, 7.5 Hz, 1H), 5.04 (dd, J = 12.5, 8.0 Hz, 1H). HRMS Calcd for $C_{20}H_{16}N_2O_2S$ $[M]^+$ 348.0932, found 348.0957

4.1.6.31. 3-(1-(furan-2-yl)-2-nitroethyl)-2-phenyl-1H-indole (63). The final compound was prepared using commercially available 2-phenylindole and **28**. Yield: 89%; ^{1}H NMR ($CDCl_3$, 500 MHz): δ 8.16 (s, 1H), 7.56 (d, J = 8.0 Hz, 1H), 7.54–7.48 (m, 4H), 7.45 (tt, J = 7.0, J = 3.0 Hz 1H), 7.39 (d, J = 8.0 Hz, 1H), 7.37 (d, J = 2.0 Hz, 1H), 7.22 (t, J = 7.5 Hz, 1.0 Hz, 1H), 7.12 (t, J = 7.5 Hz, 1H), 6.32–6.28 (m, 1H), 6.14 (d, J = 3.5 Hz, 1H), 5.36 (t, J = 7.5 Hz, 1H), 5.23 (dd, J = 12.5, 8.0 Hz, 1H), 4.94 (dd, J = 12.5, 8.0 Hz, 1H). HRMS Calcd for $C_{20}H_{16}N_2O_3$ $[M]^+$ 332.1161, found 332.1166

4.1.6.32. 3-(1-(furan-3-yl)-2-nitroethyl)-2-phenyl-1H-indole (64). The final compound was prepared using commercially available 2-phenylindole and **29**. Yield: 74%; ^{1}H NMR ($CDCl_3$, 500 MHz): δ 8.09 (s, 1H), 7.46 (d, J = 7.5 Hz, 1H), 7.43–7.38 (m, 5H), 7.35 (d, J = 8.0 Hz, 1H), 7.31 (t, J = 1.5 Hz, 1H), 7.21 (d, J = 1.0 Hz, 1H), 7.17 (t, J = 7.5 Hz, 1H), 7.07 (t, J = 7.5 Hz, 1H), 6.25 (d, J = 1.0 Hz, 1H), 5.11 (t, J = 7.5, 1.0 Hz, 1H), 5.03 (dd, J = 12.5, 8.5 Hz, 1H), 4.89 (dd, J = 12.0, 8.0 Hz, 1H). HRMS Calcd for $C_{20}H_{16}N_2O_3$ $[M]^+$ 332.1161, found 332.1176

4.1.6.33. 3-(2-nitro-1-(1H-pyrrol-2-yl)ethyl)-2-phenyl-1H-indole (65). The final compound was prepared using commercially available 2-phenylindole and **30**. Yield: 15%; ^{1}H NMR (500 MHz, $(CD_3)_2SO$): δ 11.38 (s, 1H), 10.59 (s, 1H), 7.57–7.51 (m, 4H), 7.45 (d, J = 8.5 Hz, 2H), 7.37 (d, J = 8.5 Hz, 1H), 7.09 (t, J = 7.5 Hz, 1H), 6.95 (t, J = 7.5, 1.0 Hz, 1H), 6.64–6.60 (m, 1H), 5.95–5.91 (m, 1H), 5.91 (s, 1H), 5.31 (dd, J = 16.0, 11.0 Hz, 1H), 5.22–5.18 (m, 2H) HRMS Calcd for $C_{20}H_{17}N_3O_2$ $[M]^+$ 331.1321, found 331.1332

4.1.6.34. 2-(2-nitro-1-(2-phenyl-1H-indol-3-yl)ethyl)thiazole (66a). The final compound was prepared using commercially available 2-phenylindole and **31a**. Yield: 82%; ^{1}H NMR (399 MHz, $CDCl_3$) δ: 8.24 (s, 1H), 7.74 (d, J = 3.2 Hz, 1H), 7.60 – 7.45 (m, 5H), 7.40 (t, J = 8.3 Hz, 2H), 7.26 – 7.19 (m, 2H), 7.08 (t, J = 7.6 Hz, 1H), 5.69 (dd, J = 13.1, 7.5 Hz, 1H), 5.61 (t, J = 7.3 Hz, 1H), 5.03 (dd, J = 13.1, 7.1 Hz, 1H). HRMS Calcd for $C_{19}H_{16}N_3O_2S$ $[M+H]^+$ 350.0958, found 350.0930

4.1.6.35. 2-(1-(6-methyl-2-phenyl-1H-indol-3-yl)-2-nitroethyl)thiazole (66b). The final compound was prepared using 6-methyl-2-phenylindole, **32**, and **31a**. Yield: 80%; ^{1}H NMR (500 MHz, $CDCl_3$) δ: 8.10 (s, 1H), 7.72 (d, J = 3.3 Hz, 1H), 7.58 – 7.54 (m, 2H), 7.54 – 7.49 (m, 2H), 7.49 – 7.43 (m, 1H), 7.28 – 7.26 (m, 1H), 7.23 (d, J = 3.3 Hz, 1H), 7.19 (s, 1H), 6.93 – 6.89 (m, 1H), 5.67 (dd, J = 13.1, 7.5 Hz, 1H), 5.58 (t, J = 7.4 Hz, 1H), 5.02 (dd, J = 13.2, 7.4 Hz, 1H), 2.44 (s, 3H). HRMS Calcd for $C_{20}H_{18}N_3O_2S$ $[M+H]^+$ 364.1114, found 364.1137

4.1.6.36. 2-(2-nitro-1-(2-phenyl-1H-indol-3-yl)ethyl)oxazole (67a). The final compound was prepared using commercially available 2-phenylindole and **31b**. Yield: 85%; ^{1}H NMR (500 MHz, $(CD_3)_2SO$) δ:

11.58 (s, 1H), 7.99 (d, J = 0.8 Hz, 1H), 7.72 – 7.68 (m, 2H), 7.59 (t, J = 7.7 Hz, 2H), 7.52 – 7.46 (m, 1H), 7.43 (d, J = 8.0 Hz, 1H), 7.39 – 7.35 (m, 1H), 7.19 (d, J = 0.8 Hz, 1H), 7.10 (ddd, J = 8.1, 7.2, 1.2 Hz, 1H), 6.96 (ddd, J = 8.3, 7.1, 1.1 Hz, 1H), 5.62 – 5.53 (m, 1H), 5.35 – 5.26 (m, 2H). HRMS Calcd for $C_{19}H_{16}N_3O_3$ $[M+H]^+$ 334.1186, found 334.1162

4.1.6.37. 2-(1-(6-methyl-2-phenyl-1H-indol-3-yl)-2-nitroethyl)oxazole (67b). The final compound was prepared using 6-methyl-2-phenylindole, **32**, and **31b**. Yield: 72%; ^{1}H NMR (500 MHz, $(CD_3)_2SO$) δ: 11.42 (s, 1H), 8.00 (d, J = 0.8 Hz, 1H), 7.73 – 7.67 (m, 2H), 7.62 – 7.56 (m, 2H), 7.52 – 7.46 (m, 1H), 7.32 (d, J = 8.2 Hz, 1H), 7.20 (d, J = 0.8 Hz, 1H), 7.16 (s, 1H), 6.83 – 6.79 (m, 1H), 5.60 – 5.53 (m, 1H), 5.33 – 5.26 (m, 2H), 2.36 (s, 3H). HRMS Calcd for $C_{20}H_{18}N_3O_3$ $[M+H]^+$ 348.1343, found 364.1341

4.1.6.38. 3-(1-(1-methyl-1H-imidazol-2-yl)-2-nitroethyl)-2-phenyl-1H-indole (68). The final compound was prepared using commercially available 2-phenylindole and **31c**. Yield: 17%; ^{1}H NMR (500 MHz, $CDCl_3$) δ: 8.24 (s, 1H), 7.58 – 7.50 (m, 5H), 7.50 – 7.45 (m, 1H), 7.36 (d, J = 8.1 Hz, 1H), 7.22 – 7.16 (m, 1H), 7.05 (t, J = 7.6 Hz, 1H), 6.96 – 6.92 (m, 1H), 6.66 – 6.62 (m, 1H), 5.81 (dd, J = 13.4, 9.1 Hz, 1H), 5.31 (dd, J = 9.1, 5.9 Hz, 1H), 4.99 (dd, J = 13.4, 5.9 Hz, 1H), 3.04 (s, 3H). HRMS Calcd for $C_{20}H_{19}N_4O_2$ $[M+H]^+$ 347.1503, found 347.1481

4.1.6.39. 3-(1-(1-methyl-1H-imidazol-4-yl)-2-nitroethyl)-2-phenyl-1H-indole (69). The final compound was prepared using commercially available 2-phenylindole and **31d**. Yield: 87%; ^{1}H NMR (399 MHz, $CDCl_3$) δ: 8.18 (s, 1H), 7.60 (d, J = 8.0 Hz, 1H), 7.57 – 7.51 (m, 2H), 7.51 – 7.45 (m, 2H), 7.45 – 7.36 (m, 3H), 7.24 – 7.18 (m, 1H), 7.09 (t, J = 7.6 Hz, 1H), 6.56 (s, 1H), 5.44 (dd, J = 12.5, 6.9 Hz, 1H), 5.29 (t, J = 7.7 Hz, 1H), 5.01 (dd, J = 12.4, 8.6 Hz, 1H), 3.57 (s, 3H). HRMS Calcd for $C_{20}H_{19}N_4O_2$ $[M+H]^+$ 347.1503, found 347.1514

4.1.6.40. 3-(1-(1-methyl-1H-imidazol-5-yl)-2-nitroethyl)-2-phenyl-1H-indole (70). The final compound was prepared using commercially available 2-phenylindole and **31e**. Yield: 68%; ^{1}H NMR (399 MHz, $(CD_3)_2SO$) δ: 11.50 (s, 1H), 7.69 – 7.55 (m, 5H), 7.50 (t, J = 7.1 Hz, 1H), 7.39 – 7.32 (m, 2H), 7.14 – 7.05 (m, 2H), 6.95 (t, J = 7.5 Hz, 1H), 5.56 (dd, J = 13.4, 9.2 Hz, 1H), 5.48 (dd, J = 13.6, 6.9 Hz, 1H), 5.15 (t, J = 8.1 Hz, 1H), 2.95 (s, 3H). HRMS Calcd for $C_{20}H_{19}N_4O_2$ $[M+H]^+$ 347.1503, found 347.1471

4.2. Activity profiling

4.2.1. Cell culture

HitHunter® (cAMP) and PathHunter® (β-arrestin2) CHO-K1 cells stably expressing hCB1R from DiscoveRx® (Eurofins, Fremont, CA) were maintained between passage 5–35 at 37 °C under 5% CO_2-95% air in F-12 DMEM (Corning Cellgro, Manassas, VA) containing 10% FBS and 1% penicillin–streptomycin with 800 μg/mL geneticin (HitHunter®) or 800 μg/mL geneticin and 300 μg/mL hygromycin B (PathHunter®). HitHunter® and PathHunter® hCB1R-CHO-K1 cells were used for data presented in Table 1.

4.2.2. HitHunter® cAMP assay

Forskolin-stimulated cAMP production by hCB1R-CHO-K1 cells was quantified using the DiscoveRx® HitHunter® assay. Cells (20,000 cells/well in low-volume 96-well plates) were incubated overnight in Opti-MEM (Invitrogen, Carlsbad, CA) containing 1% FBS at 37 °C under a humidified 5% CO_2-95% air atmosphere. For test-compound profiling, the Opti-MEM media was removed and replaced with cAMP assay buffer (DiscoveRx), and the cells were treated at 37 °C with test agents (0.10 nM – 10 μM, final concentrations) for 30 min, then treated with 20 μM forskolin, and EC_{20} of CP55,940 for an additional 30 min. cAMP antibody solution and cAMP working detection solution were then added to cells according to the manufacturer's directions (DiscoveRx®), and cells were incubated for 60 min at room temperature in the dark. cAMP solution A was added according to the manufacturer's directions (DiscoveRx®), and cells were incubated for 3 h at room temperature in the dark before chemiluminescence was measured on a Cytation 5 plate reader (BioTek, Winooski, VT) (top read, gain 200, integration time 10,000 ms).

4.2.3. PathHunter® β-arrestin-2 assay

β-arrestin-2 recruitment was determined using the PathHunter® assay (DiscoveRx®) with hCB1R- CHO-K1 cells. The cells (20,000 cells/well in low-volume 96 well plates) were incubated overnight in Opti-MEM (Invitrogen) containing 1% FBS at 37 °C under humidified 5% CO_2-95% air. Following this, cells were incubated in this medium at 37 °C with test compounds (0.10 nM–10 μM, final concentrations.) for 30 min, then treated with EC_{20} of CP55,940, followed by an additional 90 min of incubation at 37 °C. Detection solution was then added according to the manufacturer's directions (DiscoveRx®), and the cells were incubated for 60 min at room temperature. Chemiluminescence was then measured on a Cytation 5 plate reader (top read, gain 200, integration time 10,000 ms).

4.2.4. Aqueous solubility assay

The kinetic water solubility of each tested compound was measured by using a turbidimetric assay as performed by Cyprotex (Watertown, MA). Each test compound was prepared as a 100-X concentrated stock solution in DMSO from which serial dilutions were performed to yield eight solutions with final test-compound concentrations of 1.6, 3.21, 6.25, 12.5, 25, 50, 100, and 200 μM. Each test-compound solution was introduced into a 96-well plate, then diluted 100-fold with PBS buffer (pH 7.4) and mixed. The solutions were incubated for two hours, and absorbance was then measured at 540 nm. An absorbance value > 3X standard deviation of the average blank absorption value was considered turbidity. The highest test compound concentration with no sign of turbidity was indicative of the compound's kinetic water solubility.

Declaration of Competing Interest

The authors declare that they have no known competing financial interests or personal relationships that could have appeared to influence the work reported in this paper.

Acknowledgements

This work was supported by grants from National Institutes of Health EY024717 (to G.A.T.)

Appendix A. Supplementary material

Supplementary data to this article can be found online at https://doi.org/10.1016/j.bmc.2020.115727.

References

1. Di Marzo V, Bifulco M, De Petrocellis L. The endocannabinoid system and its therapeutic exploitation. *Nat Rev Drug Discov.* 2004;3:771–784.
2. Aizpurua-Olaizola O, Elezgarai I, Rico-Barrio I, Zarandona I, Etxebarria N, Usobiaga A. Targeting the endocannabinoid system: future therapeutic strategies. *Drug Discovery Today.* 2017;22:105–110.
3. Maurya N, Velmurugan BK. Therapeutic applications of cannabinoids. *Chem Biol Interact.* 2018;293:77–88.
4. Mechoulam R, Parker LA. The Endocannabinoid System and the Brain. *Annu Rev Psychol.* 2013;64:21–47.
5. Howlett AC, Abood ME. CB1 and CB2 Receptor Pharmacology. *Adv Pharmacol.* 2017;80:169–206.
6. Tam J, Hinden L, Drori A, Udi S, Azar S, Baraghithy S. The therapeutic potential of targeting the peripheral endocannabinoid/CB1 receptor system. *Eur J Intern Med.*

2018;49:23–29.
7. Shrestha N, Cuffe JSM, Hutchinson DS, et al. Peripheral modulation of the endocannabinoid system in metabolic disease. *Drug Discov Today*. 2018;23:592–604.
8. van Eenige R, van der Stelt M, Rensen PCN, Kooijman S. Regulation of Adipose Tissue Metabolism by the Endocannabinoid System. *Trends Endocrinol Metab*. 2018;29:326–337.
9. Mazier W, Saucisse N, Gatta-Cherifi B, Cota D. The Endocannabinoid System: Pivotal Orchestrator of Obesity and Metabolic Disease. *Trends Endocrinol Metab*. 2015;26:524–537.
10. Lange MD, Daldrup T, Remmers F, et al. Cannabinoid CB1 receptors in distinct circuits of the extended amygdala determine fear responsiveness to unpredictable threat. *Mol Psychiatry*. 2017;22:1422–1430.
11. Spiacci GBL, Antero LS, Reis DG, Lisboa SF, Resstel LB. Dorsal hippocampus cannabinoid type 1 receptors modulate the expression of contextual fear conditioning in rats: Involvement of local glutamatergic/nitrergic and GABAergic neurotransmissions. *Eur Neuropsychopharmacol*. 2016;26:1579–1589.
12. H. Chung, A. Fierro, C.D. Pessoa-Mahana, Cannabidiol binding and negative allosteric modulation at the cannabinoid type 1 receptor in the presence of delta-9-tetrahydrocannabinol: An In Silico study, PLoS One, 14 (2019) e0220025-e0220025.
13. Shore DM, Baillie GL, Hurst DH, et al. Allosteric Modulation of a Cannabinoid G Protein-coupled Receptor: Binding site elucidation and relationship to g protein signaling. *J Biol Chem*. 2014;289:5828–5845.
14. Christopoulos A, Kenakin T. G Protein-Coupled Receptor Allosterism and Complexing. *Pharmacol Rev*. 2002;54:323.
15. Janero DR, Thakur GA. Leveraging allostery to improve G protein-coupled receptor (GPCR)-directed therapeutics: cannabinoid receptor 1 as discovery target. *Expert Opin Drug Discov*. 2016;11:1223–1237.
16. Gao Z-G, Jacobson KA. Allosteric modulation and functional selectivity of G protein-coupled receptors. *Drug Discov Today Technol*. 2013;10:e237–e243.
17. Keov P, Sexton PM, Christopoulos A. Allosteric modulation of G protein-coupled receptors: a pharmacological perspective. *Neuropharmacology*. 2011;60:24–35.
18. Kulkarni AR, Garai S, Janero DR, Thakur GA. Chapter Thirteen - Design and Synthesis of Cannabinoid 1 Receptor (CB1R) Allosteric Modulators: Drug Discovery Applications. In: Reggio PH, ed. *Methods in Enzymology*. Academic Press; 2017:281–315.
19. Thakur GA, Kulkarni PM. *Allosteric Modulators of CB1 Cannabinoid Receptors*. United States: Patent Cooperation Treaty; 2013.
20. Ignatowska-Jankowska BM, Baillie GL, Kinsey S, et al. A Cannabinoid CB1 Receptor-Positive Allosteric Modulator Reduces Neuropathic Pain in the Mouse with No Psychoactive Effects. *Neuropsychopharmacology*. 2015;40:2948–2959.
21. Tseng C-C, Baillie G, Donvito G, et al. The Trifluoromethyl Group as a Bioisosteric Replacement of the Aliphatic Nitro Group in CB1 Receptor Positive Allosteric Modulators. *J Med Chem*. 2019;62:5049–5062.
22. Lu D, Immadi SS, Wu Z, Kendall DA. Translational potential of allosteric modulators targeting the cannabinoid CB1 receptor. *Acta Pharmacol Sin*. 2019;40:324–335.
23. Laprairie RB, Kulkarni PM, Deschamps JR, et al. Enantiospecific Allosteric Modulation of Cannabinoid 1 Receptor. *ACS Chem Neurosci*. 2017;8:1188–1203.
24. Garai S, Kulkarni PM, Schaffer PC, et al. Application of Fluorine- and Nitrogen-Walk Approaches: Defining the Structural and Functional Diversity of 2-Phenylindole Class of Cannabinoid 1 Receptor Positive Allosteric Modulators. *J Med Chem*. 2020;63:542–568.
25. Jaladanki CK, Taxak N, Varikoti RA, Bharatam PV. Toxicity Originating from Thiophene Containing Drugs: Exploring the Mechanism using Quantum Chemical Methods. *Chem Res Toxicol*. 2015;28:2364–2376.
26. Gramec D, Peterlin Mašič L, Sollner Dolenc M. Bioactivation Potential of Thiophene-Containing Drugs. *Chem Res in Toxicol*. 2014;27:1344–1358.
27. Ritchie TJ, Macdonald SJF. Heterocyclic replacements for benzene: Maximising ADME benefits by considering individual ring isomers. *Eur J Med Chem*. 2016;124:1057–1068.
28. Hurst DP, Garai S, Kulkarni PM, Schaffer PC, Reggio PH, Thakur GA. Identification of CB1 Receptor Allosteric Sites Using Force-Biased MMC Simulated Annealing and Validation by Structure-Activity Relationship Studies. *ACS Med Chem Lett*. 2019;10:1216–1221.
29. Kuster George JT, Steeghs Ru.ud.HJ, Scheeren Hans W. Novel Five/Five- and Six/Five-Membered Bicyclic Nitroso Acetals from High-Pressure-Promoted Cyclisation Reactions of p-Methoxybenzyl Vinyl Ether, 1-Nitro-2-heteroaryl Ethenes, and Mono- and Di-Substituted Olefins. *Eur J Org Chem*. 2001(3):553–560.
30. Yang S-D, Sun C-L, Fang Z, Li B-J, Li Y-Z, Shi Z-J. Palladium-Catalyzed Direct Arylation of (Hetero)Arenes with Aryl Boronic Acids. *Angew Chem Int Ed*. 2008;47:1473–1476.
31. Al-Zoubi R, Morales P, Reggio PH. Structural Insights into CB1 Receptor Biased Signaling. *Int J Mol Sci*. 2019;20:1837.
32. Laprairie RB, Bagher AM, Rourke JL, et al. Positive allosteric modulation of the type 1 cannabinoid receptor reduces the signs and symptoms of Huntington's disease in the R6/2 mouse model. *Neuropharmacology*. 2019;151:1–12.
33. Myers AG, Barbay JK, Zhong B. Asymmetric Synthesis of Chiral Organofluorine Compounds: Use of Nonracemic Fluoroiodoacetic Acid as a Practical Electrophile and Its Application to the Synthesis of Monofluoro Hydroxyethylene Dipeptide Isosteres within a Novel Series of HIV Protease Inhibitors. *J Am Chem Soc*. 2001;123:7207–7219.
34. Shipps GWDY, Cooper AB, Binyuan S, Wang J, Zhu L. *Fused pyrazole derivatives as novel erk inhibitors. W.I.P. Organization*. United States: Patent Cooperation Treaty; 2012.
35. Sudhakar Chary V, Rajanna KC, Krishnaiah G, Srinivas P. Zeolite Y-assisted nitration of aromatic and heterocyclic compounds and decarboxylative nitration of α, β-unsaturated acids under non-conventional conditions. *Catal Sci Technol*. 2016;6:1430–1434.
36. Trost BM, Müller C. Asymmetric Friedel−Crafts Alkylation of Pyrroles with Nitroalkenes Using a Dinuclear Zinc Catalyst. *J Am Chem Soc*. 2008;130:2438–2439.
37. Midya SP, Rana J, Abraham T, Aswin B, Balaraman E. Metal-free radical trifluoromethylation of β-nitroalkenes through visible-light photoredox catalysis. *Chem Commun*. 2017;53:6760–6763.
38. Zhang C, Li J, Tian J, et al. (1R,2R)-(+)-(1,2)-DPEN-Bonded Sulfonic Acid Resin: A Trifunctional Heterogeneous Catalyst for Asymmetric Michael Additions of Acetone to Nitroolefins. *Synth Commun*. 2015;45:1248–1258.
39. Andrey O, Alexakis A, Bernardinelli G. Asymmetric Michael Addition of α-Hydroxyketones to Nitroolefins Catalyzed by Chiral Diamine. *Org Lett*. 2003;5:2559–2561.
40. Han Y-Y, Han W-Y, Hou X, Zhang X-M, Yuan W-C. FeCl3-Catalyzed Stereoselective Construction of Spirooxindole Tetrahydroquinolines via Tandem 1,5-Hydride Transfer/Ring Closure. *Org Lett*. 2012;14:4054–4057.
41. Chen H, Han X, Qin N, et al. Synthesis and biological evaluation of novel inhibitors against 1,3,8-trihydroxynaphthalene reductase from Magnaporthe grisea. *Bioorg Med Chem*. 2016;24:1225–1230.
42. Xu C, Du J, Ma L, Li G, Tao M, Zhang W. Tertiary amine functionalized polyacrylonitrile fiber catalyst for the synthesis of tetrahydrothiophenes. *Tetrahedron*. 2013;69:4749–4757.
43. Zhao A, Jiang Q, Jia J, et al. K2S2O8-mediated nitration of alkenes with NaNO2 and 2,2,6,6-tetramethylpiperidine-1-oxyl: stereoselective synthesis of (E)-nitroalkenes. *Tetrahedron Lett*. 2016;57:80–84.
44. Abdel-Fattah MAO, Abadi AH, Lehmann J, Schweikert PM, Enzensperger C. D1-like receptors distinguishing thieno-azecine regioisomers. *MedChemComm*. 2015;6:1679–1686.
45. Poomathi N, Perumal PT. Cinchona alkaloid and di-tert-butyldicarbonate–DMAP promoted efficient synthesis of (E)-nitroolefins. *RSC Adv*. 2016;6:54495–54502.
46. Haginoya N, Kobayashi S, Komoriya S, et al. Synthesis and Conformational Analysis of a Non-Amidine Factor Xa Inhibitor That Incorporates 5-Methyl-4,5,6,7-tetrahydrothiazolo[5,4-c]pyridine as S4 Binding Element. *J Med Chem*. 2004;47:5167–5182.
47. Strachan J-P, O'Shea DF, Balasubramanian T, Lindsey JS. Rational Synthesis of Meso-Substituted Chlorin Building Blocks. *J Org Chem*. 2000;65:3160–3172.